

Modelling of the electrodiffusion process for the ion exchange in glass

M. BŁAHUT

Silesian Technical University, Institute of Physics, ul. Bolesława Krzywoustego 2, 44–400 Gliwice, Poland.

In the paper, studies of the ion-exchange technique in glass in the presence of an external electric field are presented. A new description of the process is proposed which takes into consideration the mobility dependence on the concentration of substituted ions and better fits theoretical characteristics to the experimental data. Theoretical results are verified experimentally for the electrodiffusion process of Ag^+ ions in certain types of glass. The formation of strip waveguides buried by electrodiffusion process is also considered.

1. Introduction

The ion-exchange technique is a widely used method of producing gradient waveguide structures in glass. Choosing carefully the technological conditions such as the kind of dopant ions, chemical composition of glass, mask opening dimension, time and temperature of the process it is possible to obtain single-mode and multimode, planar or strip waveguides for a wide range of geometrical dimensions and optical characteristics [1], [2]. Gradient-index waveguide structures have been applied in passive integrated optical components, in the technology of planar lightguide sensors working with phase modulation or in interference systems, made monolithically on a glass substrate plate [3]–[6]. Designing of such structures for the expected modal properties and working characteristics can be realized by mathematical modelling of the suitable ion-exchange process.

One of the basic ion-exchange processes is the diffusion in the presence of an external electric field. As shown by experimental data [1], the conformity of the experimental refractive index profiles with characteristics of the standard ion-exchange theory is dissatisfying. In the present paper, we proposed a modification of the standard electrodiffusion equation which better fits theoretical characteristics to the experimental data. The model is verified for the electrodiffusion process of Ag^+ ions in certain types of glass. Results of the theory have been applied in the modelling of the formation of strip waveguides buried by electrodiffusion process.

2. Theoretical model of the electrodiffusion process

The electrodiffusion process makes possible the fabrication of deep refractive index profiles in a short time. In this process, substituted ions (a) of the concentration n_a take the place of ions (b) of the concentration n_b which are the natural components of the glass substrate. The external electric field E_0 forces constant flow of ions in the direction from the plane of the substrate being in contact with the source of dopant ions to the external plane. The resultant flux is the sum of both fluxes of ions:

$$\begin{aligned}\bar{j}_a &= -D_a \text{grad}(n_a) + \mu_a n_a (\bar{E} + \bar{E}_0), \\ \bar{j}_b &= -D_b \text{grad}(n_b) + \mu_b n_b (\bar{E} + \bar{E}_0)\end{aligned}\quad (1)$$

where: E is the internal electric field, related to the difference of the mobility of the exchanged ions, coupling the migration of both types of ions; μ_a , D_a , μ_b , D_b denote the mobility and self-diffusion coefficients of ions, respectively.

In a steady state

$$\bar{j}_a + \bar{j}_b = \mu_b n_e \bar{E}_0 = \bar{j}_e \quad (2)$$

where: j_e is the flux of substrate ions far from the source of dopant ions, $n_e = n_a + n_b$ is the equilibrium concentration. Taking into account Eqs. (1), (2) and conditions of continuity and electric neutrality [1], an equation describing the electrodiffusion process is obtained

$$\frac{\partial N_a}{\partial t} = \text{div} \left(\frac{D_a}{1 - (1-r)N_a} \text{grad}(N_a) \right) - \text{div} \left(\frac{N_a \mu_a \bar{E}_0}{1 - (1-r)N_a} \right), \quad (3)$$

in which $N_a = n_a/n_e$ is the normalized concentration and $r = \mu_a/\mu_b$ is the mobility ratio.

Figure 1 presents a typical one-dimensional refractive index distribution profile obtained by the electrodiffusion process in borosilicate glass for the $\text{Ag}^+ - \text{Na}^+$ ion exchange [1]. Experimental points determined by the IWKB method are compared with the theory. Material parameters of the technological process – self-diffusion coefficient of Ag^+ ions D_a , the mobility ratio r and the maximum of the refractive index change are determined by measurements of respective planar diffusion profiles. Based on the above, the nonlinear electrodiffusion equation (3) is solved by an explicit finite difference scheme with appropriate initial and boundary conditions and the mobility μ_a is estimated.

A comparison of both characteristics indicates large divergence of the refractive index profiles, particularly in the region of the high concentration of substituted ions. Similar nonalignments are also observed for other types of glass [1]. This causes serious problems for the modelling of the important, for the practical application, multi-step ion-exchange processes with the use of electrodiffusion, specially for the burying by the electrodiffusion process.

The fact of the course of the electrodiffusion refractive index profiles being different from theoretical predictions can be explained by the dependence of the mobility μ_a on the concentration of substituted ions.

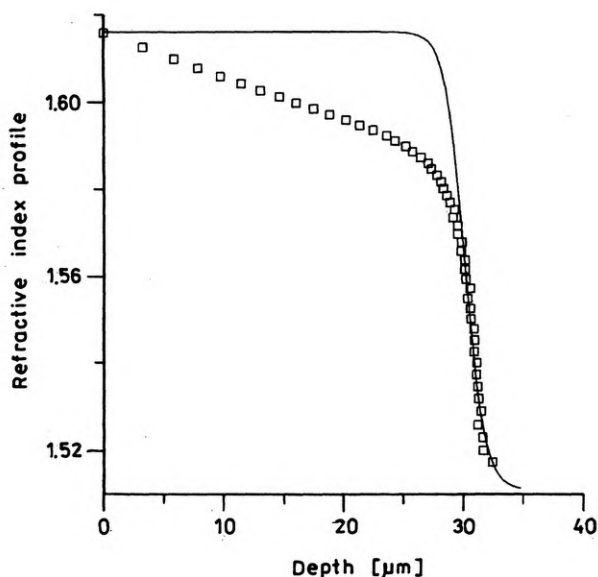


Fig. 1. Refractive index profile fabricated in borosilicate glass in the electrodiffusion process for the time $t_e = 1$ h, temperature $T = 573$ K, $E_0 = 40$ V/mm. \square – experimental points, solid line – numerical solution of Eq. (3), fitted for $\mu_a = 12.20 \times 10^2$ [$\mu\text{m}^2/\text{Vh}$]

Assuming in Equation (3) $\mu_a = \mu_a(N_a)$ the electrodiffusion equation takes the form

$$\begin{aligned} \frac{\partial N_a}{\partial t} = & \operatorname{div} \left(\frac{D_a}{1 - (1-r)N_a} \operatorname{grad}(N_a) \right) - \mu_a(N_a) \bar{E}_0 \operatorname{grad} \left(\frac{N_a}{1 - (1-r)N_a} \right) \\ & - \bar{E}_0 \left(\frac{N_a}{1 - (1-r)N_a} \right) \operatorname{grad}(\mu_a). \end{aligned} \quad (4)$$

The function $\mu_a(N_a)$ should change in the region of the high concentration N_a and become stable for low concentrations. It is assumed that it can be described by the equation

$$\mu_a(N_a) = \begin{cases} \mu_0 & \text{for } N_a < n_0, \\ \mu_0 \exp(-(N_a - n_0)^2 / \sigma^2) & \text{for } N_a > n_0 \end{cases} \quad (5)$$

where n_0 defines the beginning and σ – the rate of changes of the mobility μ_a . Both parameters are determined from the comparison of theoretical and experimental results. Figure 2 shows a typical dependence of normalized mobility $\mu_a(N_a)/\mu_0$ for $n_0 = 0.6$ and $\sigma = 0.35$.

Numerical results of refractive index profiles from the equation of electrodiffusion (4) for different parameters n_0 and σ are presented in Figs. 3, 4. One can see that the dependence of the mobility on concentration cuts down the first part of the refractive

index distribution as compared to relation similar to a step index refractive profile for $\mu_a = \text{const.}$ and generally influences the migration rate of substituted ions.

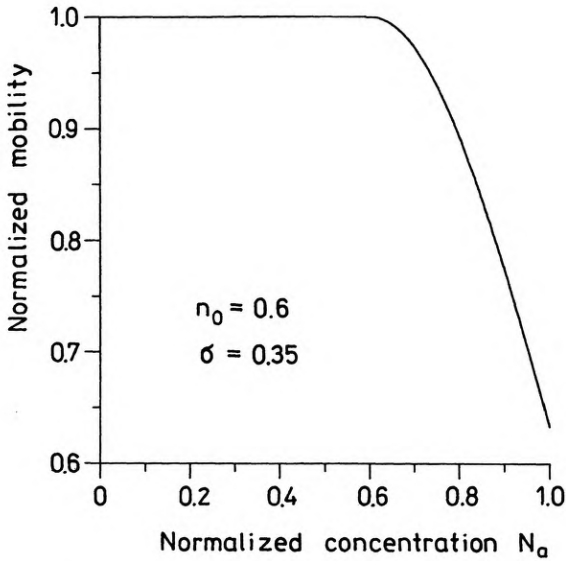


Fig. 2. Normalized mobility $\mu_a(N_a)/\mu_0$ as a function of the normalized concentration N_a for $n_0 = 0.6$ and $\sigma = 0.35$

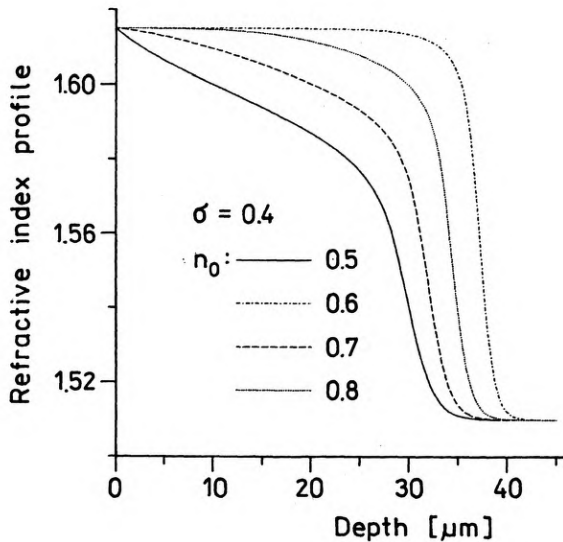


Fig. 3. Refractive index profiles after electrodiffusion (time $t_0 = 1$ h, temperature $T = 573$ K, $E_0 = 40$ V/mm) in borosilicate glass calculated numerically from Eq. (4) for $\mu_0 = 16.53 \times 10^2$ [$\mu\text{m}^2/\text{Vh}$], $\sigma = 0.4$ and different parameters n_0

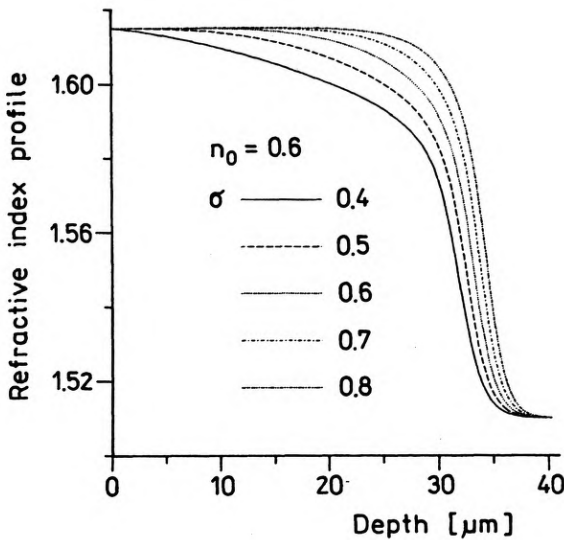


Fig. 4. Refractive index profiles after electrodiffusion (time $t_e = 1$ h, temperature $T = 573$ K, $E_0 = 40$ V/mm) in borosilicate glass calculated numerically from Eq. (4) for $\mu_0 = 16.53 \times 10^2$ [$\mu\text{m}^2/\text{Vh}$], $n_0 = 0.6$ and different parameters σ

The results obtained are used in an analysis of the electrodiffusion process of Ag^+ ions in the selected types of glass which differ in a chemical composition and in the contents of Na^+ ions, taking part in the ion exchange [1], [2]. Some technological parameters of the investigated glasses are presented in the Table.

Table. Technological parameters of selected types of glass

	NaNO ₃ contents [% mol]	D_e [$\mu\text{m}^2/\text{h}$]	r	μ_0 10^2 [$\mu\text{m}^2/\text{Vh}$]	n_0	σ
Borosilicate	15	13.4	0.45	16.53	0.6	0.35
KF-3	16.6	14.6	0.2	1.17	0.55	0.18
BK-7	8.8	2.3	0.5	1.07	0.6	0.4
Soda-lime	12.2	11.6	0.3	12.44	0.6	0.23
"Termisil"	3	7.04	1.0	4.46	0.75	0.8

Figures 5, 6 show the electrodiffusion profiles produced in borosilicate glass for the temperature $T = 300$ °C and electrical fields $E_0 = 28$ V/mm and 40 V/mm. The best fitting of theoretical curves to experimental points for each profile is obtained for the parameters $\mu_0 = 16.53 \times 10^2$ [$\mu\text{m}^2/\text{Vh}$], $n_0 = 0.6$ and $\sigma = 0.35$. Similar characteristics for the KF-3 glass [2] for the electrodiffusion in external fields $E_0 = 50$ V/mm and 102 V/mm, $T = 300$ °C and parameters $\mu_0 = 1.17 \times 10^2$ [$\mu\text{m}^2/\text{Vh}$], $n_0 = 0.55$ and $\sigma = 0.18$ are presented in Figs. 7, 8.

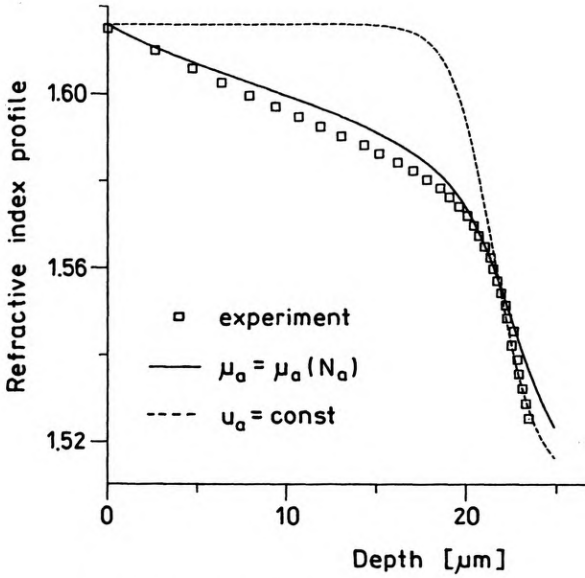


Fig. 5. Comparison of theoretical and experimental results for the electrodiffusion at time $t_e = 1$ h, temperature $T = 573$ K, $E_0 = 28$ V/mm in borosilicate glass. Numerical solution of Eq. (4) is determined for $\mu_0 = 16.53 \times 10^2$ [$\mu\text{m}^2/\text{Vh}$], $n_0 = 0.6$ and $\sigma = 0.35$. The solution for $\mu_a = \text{const}$. is fitted for $\mu_a = 12.20 \times 10^2$ [$\mu\text{m}^2/\text{Vh}$]

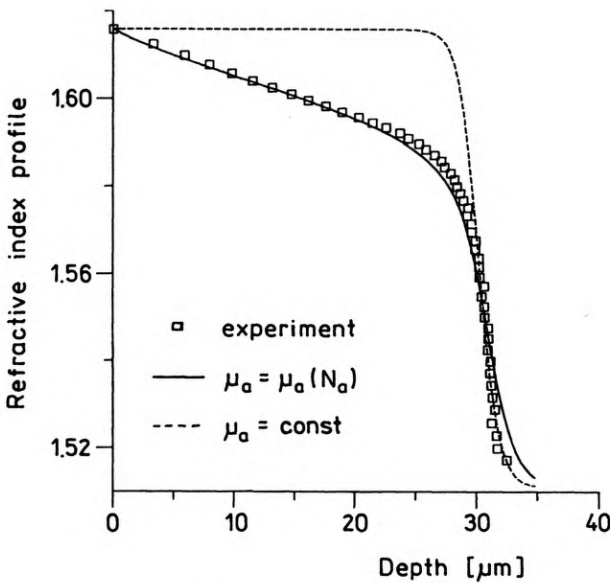


Fig. 6. Comparison of theoretical and experimental results for the electrodiffusion at time $t_e = 1$ h, temperature $T = 573$ K, $E_0 = 40$ V/mm in borosilicate glass. Numerical solution of Eq. (4) is determined for $\mu_0 = 16.53 \times 10^2$ [$\mu\text{m}^2/\text{Vh}$], $n_0 = 0.6$ and $\sigma = 0.35$. The solution for $\mu_a = \text{const}$. is fitted for $\mu_a = 12.20 \times 10^2$ [$\mu\text{m}^2/\text{Vh}$]

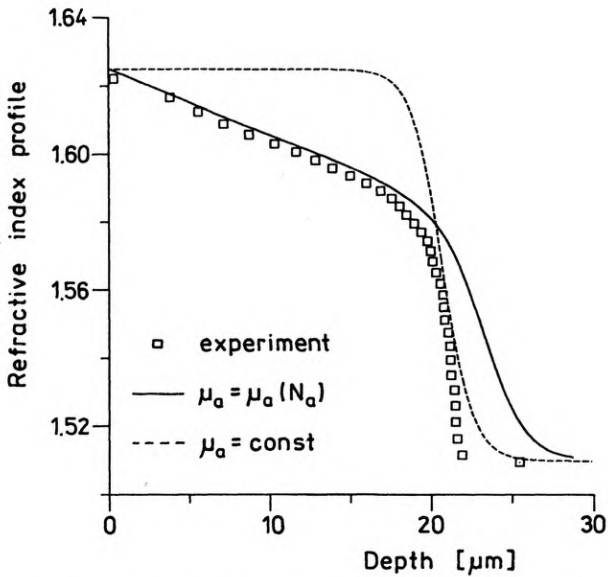


Fig. 7. Comparison of theoretical and experimental results for the electrodiffusion at time $t_e = 1$ h, temperature $T = 573$ K, $E_0 = 50$ V/mm in KF-3 glass. Numerical solution of Eq. (4) is determined for $\mu_0 = 1.17 \times 10^2$ [$\mu\text{m}^2/\text{Vh}$], $n_0 = 0.55$ and $\sigma = 0.18$. The solution for $\mu_a = \text{const}$. is fitted for $\mu_a = 0.49 \times 10^2$ [$\mu\text{m}^2/\text{Vh}$]

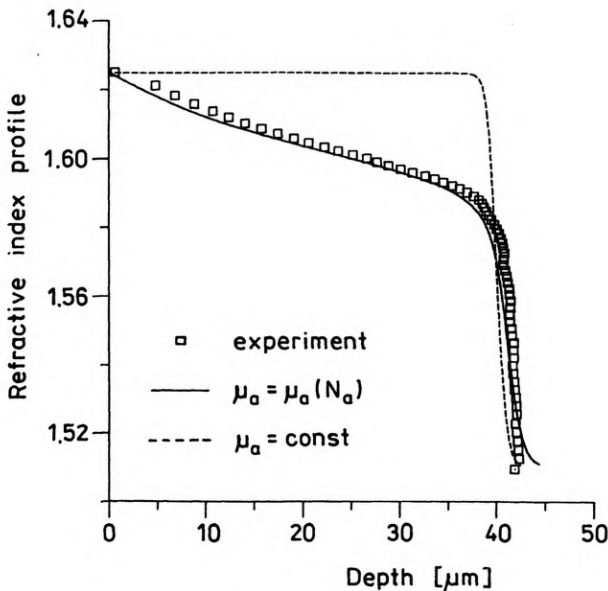


Fig. 8. Comparison of theoretical and experimental results for the electrodiffusion at time $t_e = 1$ h, temperature $T = 573$ K, $E_0 = 102$ V/mm in KF-3 glass. Numerical solution of Eq. (4) is determined for $\mu_0 = 1.17 \times 10^2$ [$\mu\text{m}^2/\text{Vh}$], $n_0 = 0.55$ and $\sigma = 0.18$. The solution for $\mu_a = \text{const}$. is fitted for $\mu_a = 0.49 \times 10^2$ [$\mu\text{m}^2/\text{Vh}$]

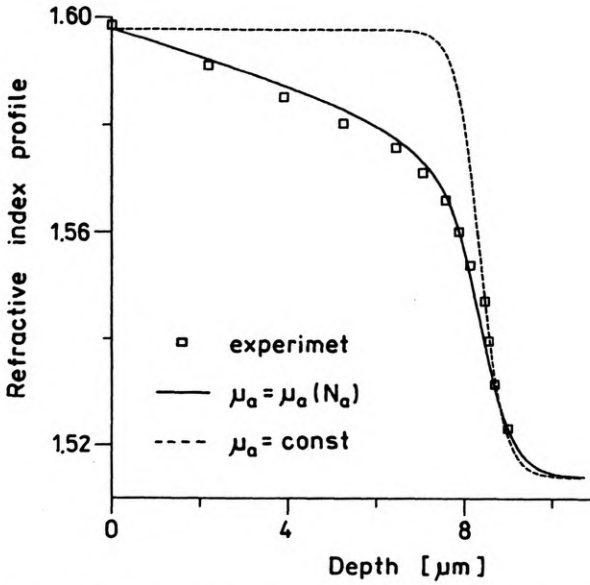


Fig. 9. Comparison of theoretical and experimental results for the electrodiffusion at time $t_s = 0.5$ h, temperature $T = 623$ K, $E_0 = 100$ V/mm in BK-7 glass. Numerical solution of Eq. (4) is determined for $\mu_0 = 1.07 \times 10^2$ [$\mu\text{m}^2/\text{Vh}$], $n_0 = 0.6$ and $\sigma = 0.4$. The solution for $\mu_s = \text{const}$ is fitted for $\mu_s = 0.88 \times 10^2$ [$\mu\text{m}^2/\text{Vh}$]

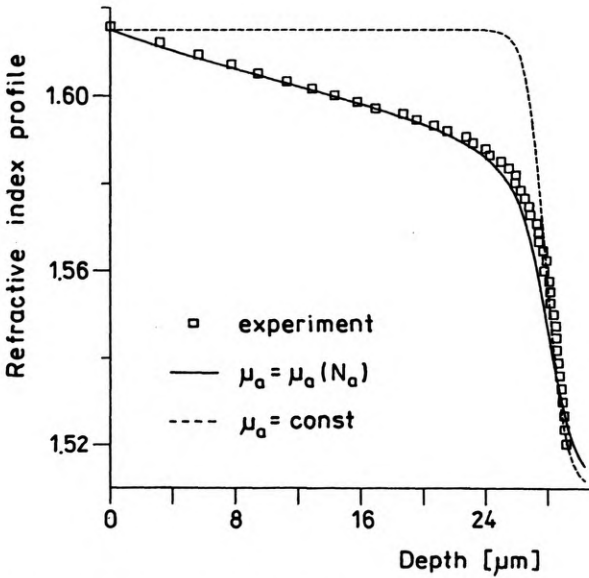


Fig. 10. Comparison of theoretical and experimental results for the electrodiffusion at time $t_s = 1$ h, temperature $T = 573$ K, $E_0 = 36$ V/mm in soda-lime glass. Numerical solution of Eq. (4) is determined for $\mu_0 = 12.44 \times 10^2$ [$\mu\text{m}^2/\text{Vh}$], $n_0 = 0.6$ and $\sigma = 0.23$. The solution for $\mu_s = \text{const}$ is fitted for $\mu_s = 7.74 \times 10^2$ [$\mu\text{m}^2/\text{Vh}$]

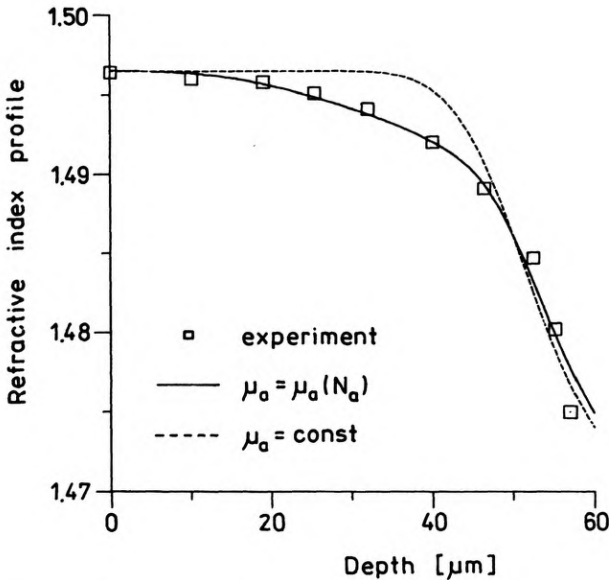


Fig. 11. Comparison of theoretical and experimental results for the electrodiffusion at time $t_e = 4$ h, temperature $T = 603$ K, $E_0 = 150$ V/mm in "Termisil" glass. Numerical solution of Eq. (4) is determined for $\mu_0 = 4.46 \times 10^2$ [$\mu\text{m}^2/\text{Vh}$], $n_0 = 0.75$ and $\sigma = 0.8$. The solution for $\mu_a = \text{const}$. is fitted for $\mu_a = 4.60 \times 10^2$ [$\mu\text{m}^2/\text{Vh}$]

In both cases a good conformity is obtained which proves that there is no dependence of the mobility parameters μ_0 , n_0 and on the external field E_0 .

The comparisons of the electrodiffusion profiles obtained in different technological conditions for the rest of glasses with the results of the theory are presented in Figs. 9, 10 and 11. The corresponding mobility parameters μ_0 , n_0 and σ are given in the Table.

3. Waveguide structures buried by the electrodiffusion

The burying by the electrodiffusion process is a popular method of producing deep and symmetrical profiles of changes of the refractive index adjusted to collaborate with optical fibers. In the two-step process, the refractive index distribution produced in the preliminary thermal diffusion of ions (a) at time t_D through the window of the width w is then separated from the glass substrate during the electrodiffusion process of ions (b) at time t_z reducing the refractive index.

The mobility dependence on the concentration influences the rate of burying. Figures 12 and 13 present two-dimensional refractive index profiles calculated numerically with appropriate initial and boundary conditions [2] for two models of burying by electrodiffusion process – for $\mu_a = \text{const}$. and $\mu_a = \mu_a(N_a)$. The process consists of the initial diffusion at time $t_D = 1$ h through the window $w = 3.7$ μm , and burying at time $t_z = 0.5$ h in the external field $E_0 = 40$ V/mm. The ion-

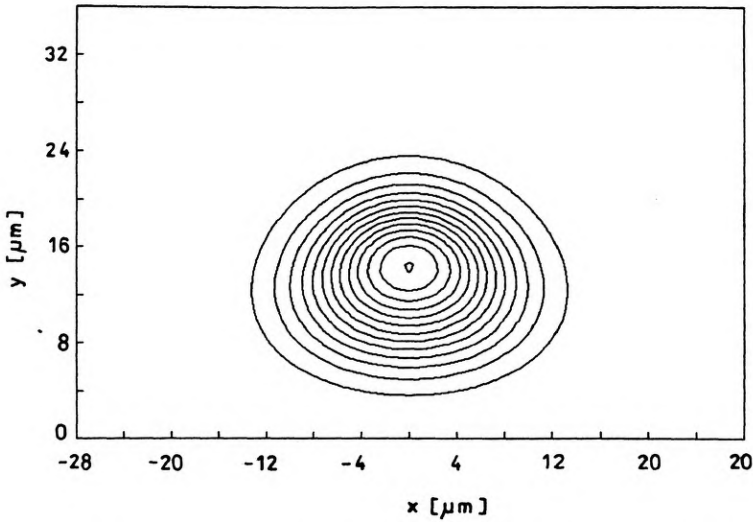


Fig. 12. Two-dimensional refractive index buried profiles calculated numerically from Eq. (4) for borosilicate glass

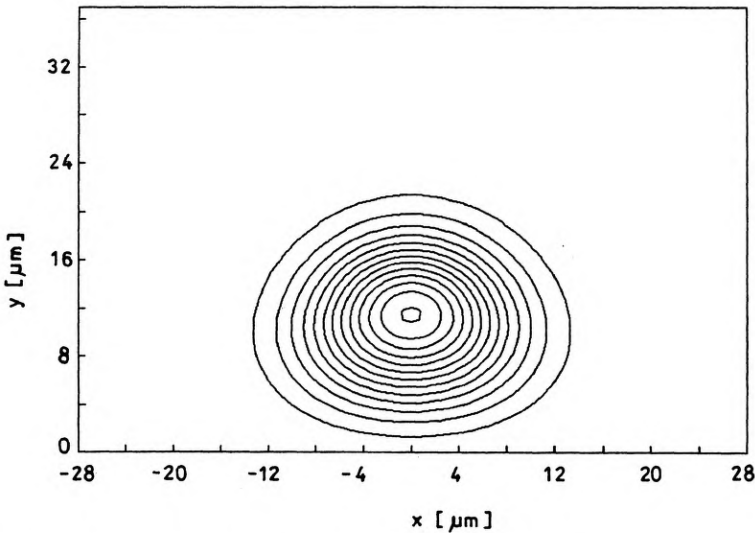


Fig. 13. Two-dimensional refractive index buried profiles calculated numerically from Eq. (3) for borosilicate glass ($\mu_s = 12.10 \times 10^2 \text{ } [\mu\text{m}^2/\text{Vh}]$)

exchange parameters and mobility parameters used in numerical simulations relate to borosilicate glass (Table). In Figure 14, the refractive index profiles $n(0, y)$ determined for the maximum of the distribution are shown. By comparing the characteristics obtained, it can be confirmed that the mobility dependence on the concentration increases the rate of burying.

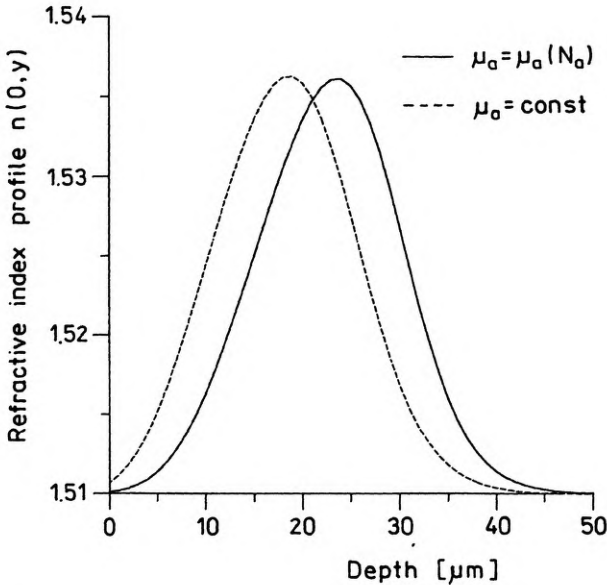


Fig. 14. Comparison of refractive index profiles $n(0, y)$ determined for the maximum of the distribution, for $\mu_a = \text{const.}$ and $\mu_a = \mu_a(N_a)$

4. Conclusions

The model of ion-exchange in the presence of an external electric field presented in this paper, assuming concentration dependent mobility of substituted ions, better fits experimental results of electrodiffusion profiles, fabricated in selected types of glass, to theoretical curves than the standard electrodiffusion equation. It has been established that the parameters describing the mobility as a function of the concentration are independent of the external electric field and in fixed temperatures they can be used in the modelling of a multi-step ion-exchange process. An analysis of burying by the electrodiffusion process shows that the assumed mobility dependence on the concentration increases the rate of burying.

The results presented will find applications in the designing of waveguide structures produced by $\text{Ag}^+ - \text{Na}^+$ ion exchange, for the expected modal properties and working characteristics.

References

- [1] BŁAHUT N., OPILSKI A., ROGOZIŃSKI R., *Opt. Appl.* **22** (1992), 161.
- [2] OPILSKI A., ROGOZIŃSKI R., BŁAHUT M., KARASIŃSKI P., GUT K., OPILSKI Z., *Opt. Eng.* **36** (1997), 1625.
- [3] BŁAHUT M., GUT K., KARASIŃSKI P., OPILSKI A., 2nd European Conf. on *Optical Chemical Sensors and Biosensors*, Florence 1994, p. 196.
- [4] BŁAHUT M., ROGOZIŃSKI R., GUT K., KARASIŃSKI P., OPILSKI A., *Opt. Appl.* **24** (1994), 171.

- [5] KARASIŃSKI P., GUT K., BŁAHUT M., OPILSKI A., *Opt. Appl.* **24** (1994), 163.
- [6] GUT K., BŁAHUT M., ROGOZIŃSKI R., KARASIŃSKI P., OPILSKI A., *Proc. SPIE* **P 29** (1996), 137.
- [7] BŁAHUT M., ROGOZIŃSKI R., *Eight CIMTEC Forum on New Materials*, Florence 1994, p. 214.

*Received October 22, 1997
in revised form January 5, 1998*